Ultrasonic Evaluation of Creep Damage in 316LN Stainless Steel

Song-Nan Yin[1], Yeong-Tak Hwang[1] and Won Yi[2,#]

1 Graduate school, Department of Mechanical Engineering, Soongsil University, Sangdo 5(o)-Dong, Dongjak-Gu, Seoul, South Korea, 156-743
2 Department of Mechanical Engineering, Soongsil University, Sangdo 5(o)-Dong, Dongjak-Gu, Seoul, South Korea, 156-743
Corresponding Author / E-mail: yiwon@ssu.ac.kr, TEL: +82-2-820-0657, FAX: +82-2-820-0668

KEYWORDS: Creep damage, Ultrasonic wave, Creep time to rupture, Wave speed, Angular frequency, Grain boundary

Creep failure of 316LN stainless steel (SS) occurs due to the nucleation and growth of cracks. An investigation was performed to correlate the creep damage with ultrasonic wave speeds and angular frequencies using creep-tested 316LN SS specimens. Ultrasonic wave measurements were made in the direction of and perpendicular to the loading using contact probes with central frequencies of 10, 15, and 20 MHz. We found that the angular frequency and wave speed decreased with increasing creep time to rupture by analyzing the ultrasonic signals from the 15 and 20 MHz probes. Therefore, the creep damage was sensitive to the angular frequency and wave speed of ultrasonic waves.

Manuscript received: March 9, 2007 / Accepted: July 9, 2007

NOMENCLATURE

ω: angular frequency
α: attenuation coefficient
c: wave speed

1. Introduction

The mechanical properties of components operating at high temperatures degrade with time. It is therefore necessary to evaluate the mechanical properties to determine the structural integrity and remnant life of the components. Material degradation must be examined periodically to avoid premature failures as it adversely affects the safety and life of the equipment and plant personnel.[1-3] Remnant life assessments usually consist of several components: using the operational history of the plant and virgin material properties to calculate the life fraction consumed, using nondestructive techniques to develop correlations between the mechanical properties and nondestructive testing parameters, and using service-exposed material removed from the component to carry out actual mechanical tests. Three nondestructive evaluation methods are usually employed: an indentation method based on the hardness, an ultrasonic method based on the physical properties of the material, and an electrical resistivity method based on changes in the electrical characteristics. Among these, the ultrasonic method has been used not only for detecting internal defects in the materials, but also for evaluating mechanical properties. Both linear and nonlinear ultrasonic methods are used. The linear ultrasonic method is based on measuring the ultrasonic wave attenuation and wave speed. This method has been employed on various materials[4-8], and the material damage has been related to the ultrasonic wave-speed reduction. The ultrasonic attenuation coefficient is especially sensitive to precipitates and the fine grain size of the material[9, 10], and the ultrasonic wave speed in a polycrystalline medium is also dependent upon the frequency of the ultrasonic wave itself.

Most studies generally use an immersion method for their ultrasonic tests, but it is difficult to immerse actual structures found in industry. Hence, we used a contact transducer to analyze the change of the ultrasonic wave speed based on a linear interpretation. We examined 316LN stainless steel (SS) with the objective of evaluating the creep damage under high temperatures.

2. Theory

2.1 Linear time-shift invariant systems

Figure 1 shows the experimental setup used in this investigation. The electric pulse from the pulser/receiver was transformed to an ultrasonic surge in a wide-band ultrasonic transducer, and then the reflected ultrasonic wave was transformed to an electric signal by the wide ultrasonic receiver. The characteristic functions in the time domain were $f(t)$, $g_1(t)$, $h(t)$, $g_2(t)$, and $x(t)$. The first reflected wave $b_1(t)$ and the second reflected wave $b_2(t)$ could be represented as a function integral. Each function in each frequency domain was also represented as a transformed Fourier function,

$$B_1(\omega) = F(\omega) \cdot G_1(\omega) \cdot H(\omega) \cdot G_2(\omega) \tag{1}$$

$$B_2(\omega) = F(\omega) \cdot G_1(\omega) \cdot H(\omega) \cdot H(\omega) \cdot G_2(\omega) \tag{2}$$

where $B_1(\omega)$, $B_2(\omega)$, $F(\omega)$, $G_1(\omega)$, $G_2(\omega)$, and $H(\omega)$ are the transformed Fourier functions of the characteristic functions. From Eqs. (1) and (2), we obtain the following clear signal,

$$\frac{B_2(\omega)}{B_1(\omega)} = H(\omega) \tag{3}$$

which was eliminated from the counter-effect of the pulser/receiver and wide ultrasonic sensor.

A moving ultrasonic wave has two wave-speed components: the circular or angular wave speed, and the linear wave speed, often referred to as just the wave speed. The angular frequency is the proceeding speed of the wave, and the wave speed is the wave energy speed in the limit of a composite wave. Speed dispersion exists inside materials since they inevitably have lattice defects. Hence, wider wave bands produce wider pulses. The wave shape also changes since the speed of sound speed is influenced by the frequency. For material degradation, the wave speed is more dependent on the frequency due to nonhomogeneities in the distribution of the defects such as voids, precipitates, and elemental segregation. Therefore, it is more important to focus on the dependency of the frequency of each wave speed when the ultrasonic wave speed is used to evaluate materials. The time of the wave travel t_0 is

$$t_0 = \frac{\arg[H(\omega)]}{\omega} \tag{4}$$

which represents two reflected waves in the frequency range, and can be used to calculate the angular frequency.

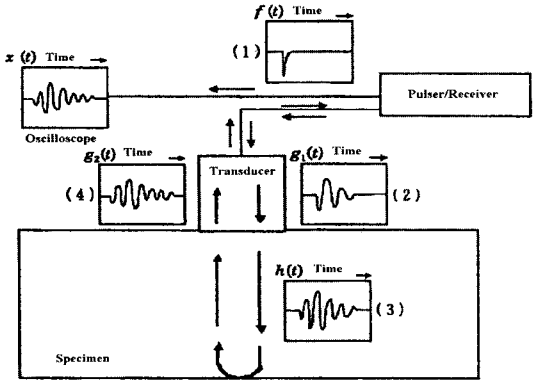

Fig. 1 Principles of the pulse echo method used for the ultrasonic analysis

2.2 Sources of attenuation

Consider a plane wave traveling in the positive z direction in a single medium. If we let A_0 be the amplitude of this wave at $z = z_0$ and A_1 be the amplitude at $z = z_1$, where $z_1 > z_0$, then in general, $A_1 < A_0$ due to losses in the propagating medium. To account for these losses, we write

$$\frac{A_1}{A_0} = \exp[-\alpha(f)\Delta z] \tag{5}$$

where $\Delta z = z_1 - z_0$ is the distance traveled and $\alpha(f)$ is a frequency-dependent attenuation coefficient.[9]

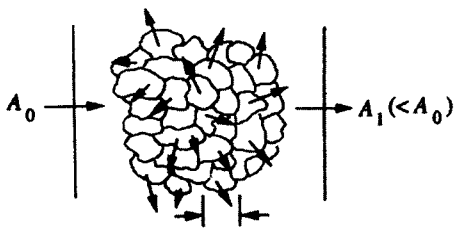

Fig. 2 Attenuation of a wave due to grain scattering

In general, several sources of attenuation exist in materials, including grain scattering and absorption. Grain-scattering losses arise because metals are composed of small crystalline grains on a microstructural level (see Fig. 2) that scatter the incident waves in many different directions, resulting in a net loss of amplitude with distance in the propagation noise. The attenuation coefficient for grain scattering depends strongly on the size of the wavelength λ relative to the average grain diameter.

Consider the one-dimensional wave equation for a fluid that includes a viscous damping term,

$$\frac{\partial^2 p}{\partial z^2} - \frac{\kappa}{c_f^2}\frac{\partial p}{\partial t} - \frac{1}{c_f^2}\frac{\partial^2 p}{\partial t^2} = 0 \tag{6}$$

where κ is a damping term and c_f is the wave speed (without damping) of the fluid. If we assume that the pressure p is characterized by an exponentially damped harmonic plane wave propagating in the positive z direction,

$$p = \exp(-\alpha z)\exp(ikz - i\omega t) \tag{7}$$

If we use this expression in Eq. (6), we find that to satisfy the damped wave equation, we must have

$$\alpha^2 - k^2 = \frac{-\omega^2}{c_f^2} \tag{8}$$

$$2\alpha k = \frac{\kappa\omega}{c_f^2} \tag{9}$$

where the wave number k and wave speed c are related by $k = \omega/c$ so that the wave speed is dependent on frequency according to

$$c = \frac{\sqrt{2}c_f}{(1+\sqrt{1+k^2/\omega^2})^{1/2}} \tag{10}$$

3. Experiment

Table 1 shows the chemical composition of 316LN SS. This material was manufactured using the vacuum induction melting process. The ingot was soaked for 2 h at 1270°C in argon and then hot rolled into 15-mm-thick plates. The rolled plates were solution-treated at 1100°C for 1 h and subsequently quenched in water.

Table 1 Chemical components of 316LN stainless steel

Fe	C	Si	Mn	P	S	Cr	Ni	Mo	N	B
Bal.	0.022	0.7	1.01	0.029	0.005	17.15	12.3	2.35	0.094	0.003

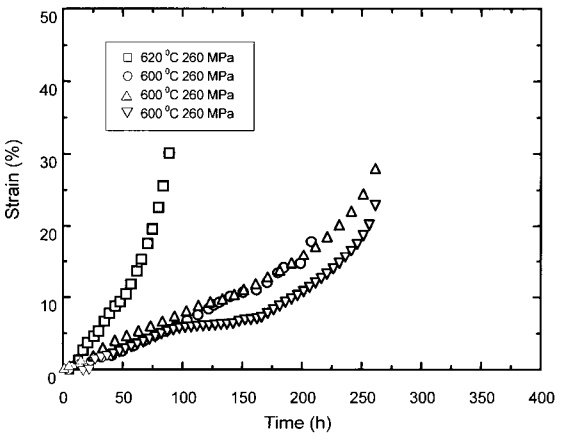

Fig. 3 Relationship between creep time and strain

The creep specimens used in this study had a nonconventional cross section to facilitate ultrasonic measurements. The specimens were initially machined as round specimens. The gage portion was then subsequently machined to provide two parallel flat faces so that the ultrasonic transducer would be in perfect contact with the specimen. The gage section had length of 30 mm, a thickness of 3 mm across the flat surfaces, and a diameter of 6 mm across the curved shape. Constant-load creep tests were performed according to the ASTM E139 standard at 600°C and several stress levels. The creep testing was conducted after the specimen was heated to 600°C for over 2 h. The elongation was measured using an extensometer that was attached to the specimen along with a LVDT, and the measured data were automatically recorded by a computer. Table 2 shows the specimen dimensions before testing and the rupture lives. Figure 3 compares the creep curves at various stress levels.

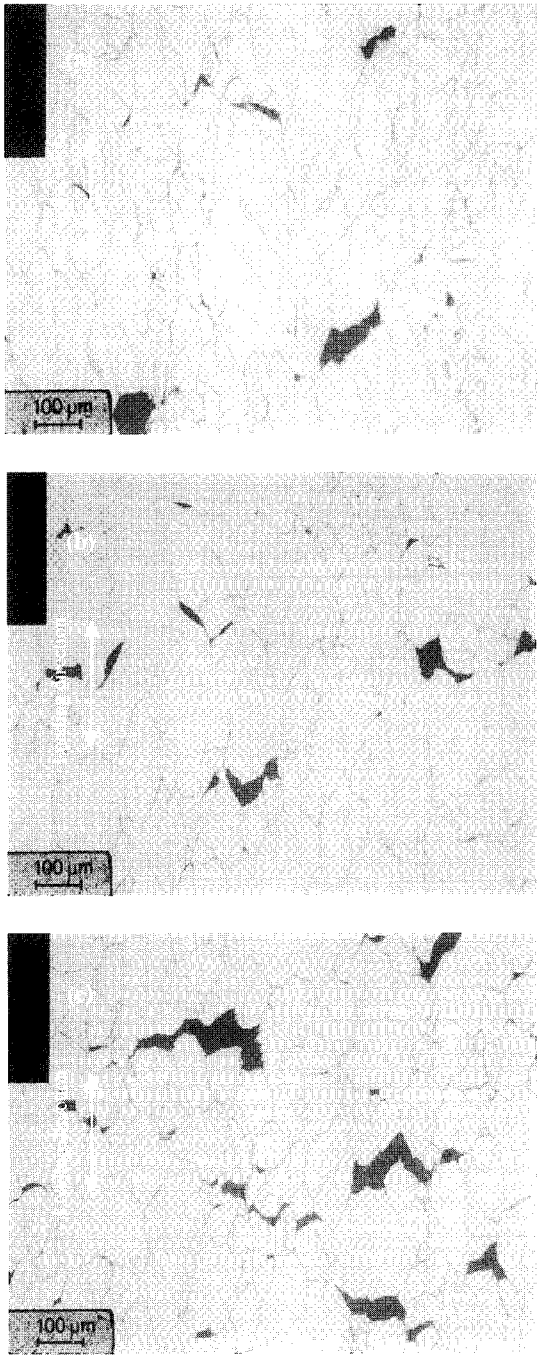

Fig. 4 Optical photographs of the creep microstructures in specimens tested under uniaxial tension showing the creep cavity increase and grain deformation decrease just before rupture. The test conditions were (a) 620°C and 260 MPa, (b) 600°C and 260 MPa, and (c) 600°C and 240 MPa

Table 2 Dimensions of an ultrasonic test specimen

Time to rupture (h)	94	215	270	260	403	284
Length (mm)	7.720	7.699	7.694	7.767	7.758	7.715
Thickness (mm)	2.258	2.308	2.310	2.495	2.526	2.508

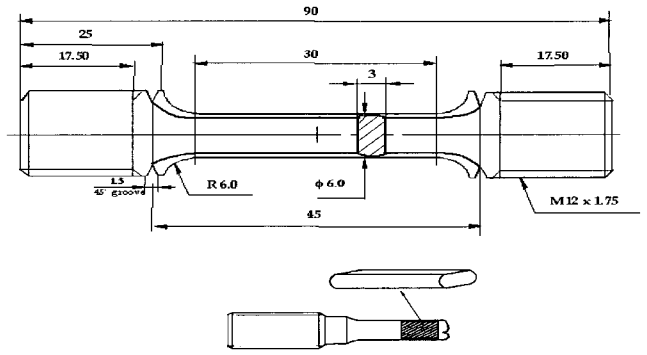

Fig. 5 Dimensions of the creep specimens and shape of the ultrasonic test specimens

4. Results and Discussion

4.1 Metallographic analysis

Metallographic studies were performed on the fractured specimen to reveal the extent of the creep damage. Figure 4 shows micrographs of specimens tested under several conditions: (a) 620°C and 260 MPa, (b) 600°C and 260 MPa, and (c) 600°C and 240 MPa. The times to rupture were 93.5, 284.0, and 403.0 h, respectively. The loading direction is indicated in the micrographs. Creep cracks were observed in all the specimens. The amount of creep damage increased and the grain deformation decreased as the creep time increased; this occurred because the creep breaks were at locations of high stresses where the fracture mode changed from intergranular to transgranular.[11, 12] The cracks were generally oriented perpendicular to the loading direction.

4.2 Creep damage evaluation using ultrasonic waves

The angular frequency and wave speed were measured by generating incident waves in the direction of and perpendicular to the loading. The 8-mm-long specimens were cut from the creep-ruptured pieces of the previous test as shown in Fig. 5. Because the contact surface of the contact transducer affects the measurements, the testing specimen was polished to a 1 μm roughness. An ultrasonic transducer was attached to the specimen surface and the signal was measured in the longitudinal and transverse directions to minimize errors. Table 2 shows the dimensions of the specimens.

Three ultrasonic transducers with center frequencies of 10 MHz (probe diameter φ = 10 mm), 15 MHz (φ = 6 mm), and 20 MHz (φ = 3 mm), and a JSR PR35 pulser/receiver were used in this experiment. A Lecroy 9354A digital oscilloscope was used at a sampling frequency of 500 MHz to display the signal received from the pulser/receiver. The oscilloscope data were recorded by a computer in real time. Glycerin was used as a coupling medium between the sample and the probe.[13, 14]

4.2.1 Evaluation in the longitudinal direction

Figure 6(a) shows the waveform of the first reflected signal obtained from the specimen that fractured after 93.5 h. The figure consists of a plot of the signal amplitude in dB versus time in microseconds, where t_1 and t_2 are the start and end times for 4π radians in the time domain. Similar plots for the specimens that were creep-tested for 262 and 403 h are shown in Figs. 6(b) and 6(c),

respectively. The angular frequency was calculated from $\omega = 2n\pi/(t_2 - t_1)$.

Figure 7 shows the variation of the angular frequency with creep time to rupture at the three different frequency levels. The angular frequency did not change with the creep time to rupture when the measurements was made using the 10-MHz probe. However, as shown in Figs. 7(b) and 7(c), the angular frequency decreased with increasing creep rupture time when the measurements were made using the 15- and 20-MHz transducers. These results are similar to those obtained from other studies.[9] The angular frequency using the 10-MHz probe probably remained unchanged due to the large diameter of the transducer, which resulted in excessive noise. The above results suggest that it is possible to evaluate the creep damage based on the angular frequency results from the 15- and 20-MHz transducers.

If the tested specimen is regarded as an elastic rod, and the edges are free, the incident surge variables are reflected back from the edges at the original wave size and phase based on wave theory.

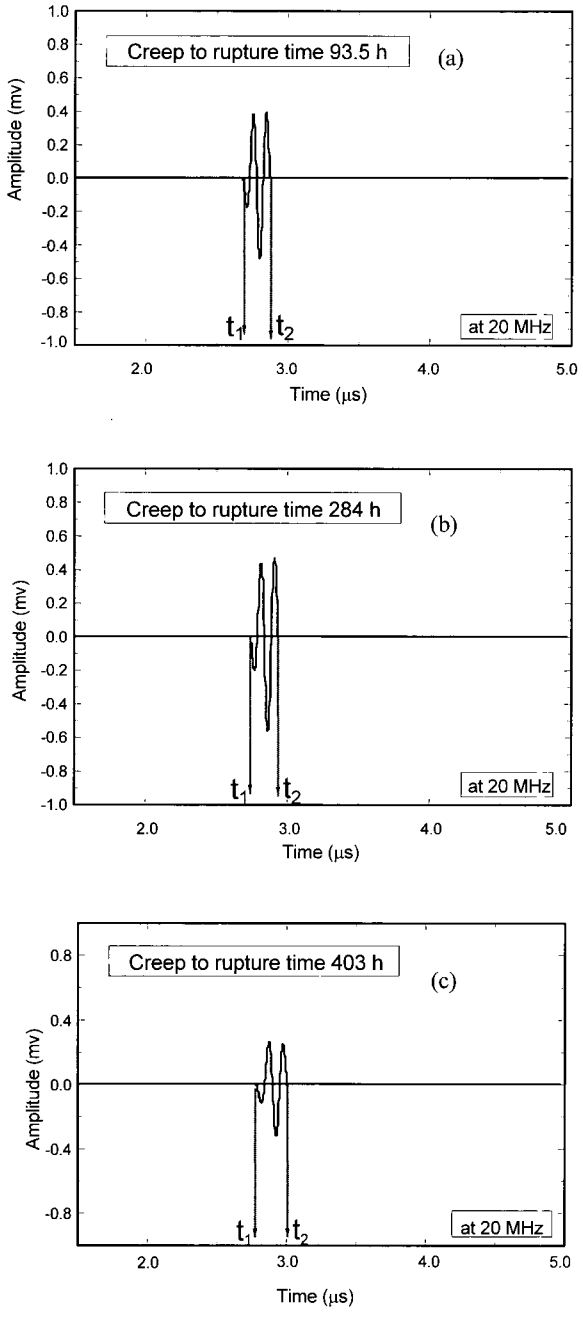

Fig. 6 First reflected waves of the ultrasonic signal from the 20-MHz transducer

The wave speed can be obtained from the reflected wave and the propagation time can be obtained from the time between the leading edge of the incident and the reflected waves. The wave speed decreased with increasing creep time to rupture, as shown in Fig. 8.

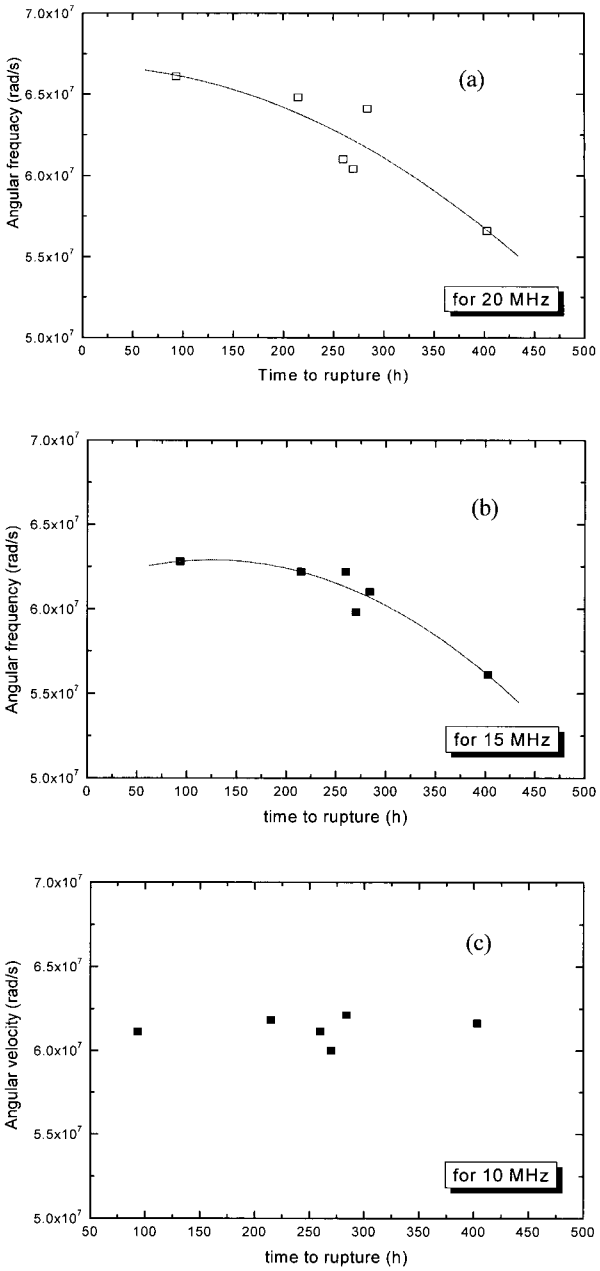

Fig. 7 Relationship between the angular frequency and the time to rupture using the 10-, 15-, and 20-MHz transducers

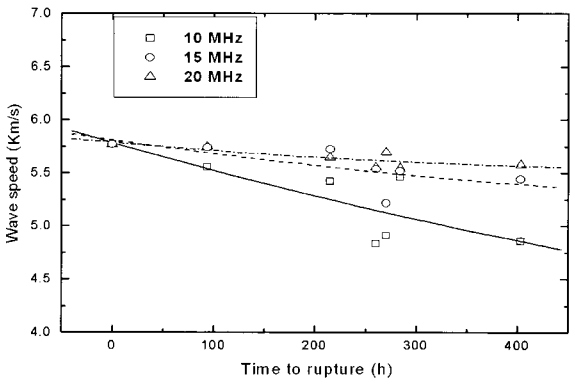

Fig. 8 Relationship between the wave speed and the time to rupture in the loading direction

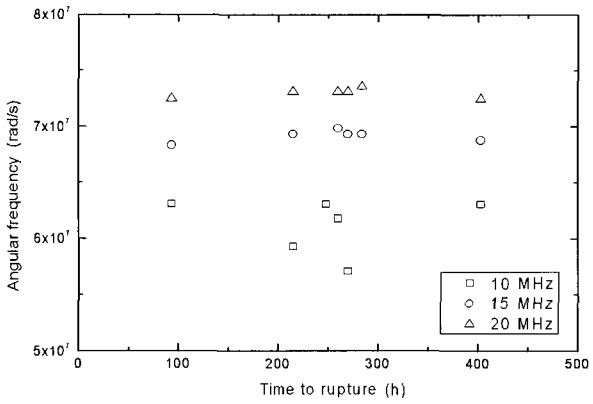

Fig. 9 Relationship between the angular frequency and the time to rupture in the perpendicular direction

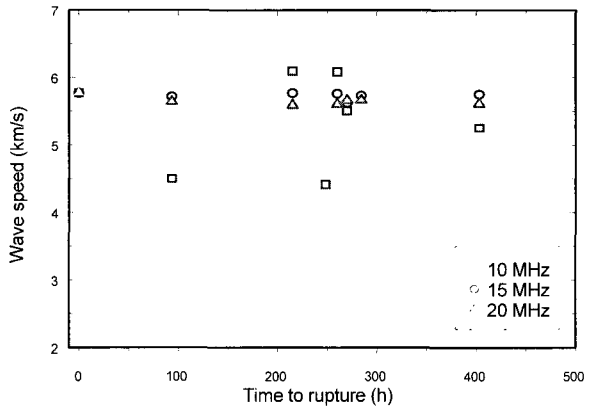

Fig. 10 Relationship between the wave speed and the time to rupture in the perpendicular direction

4.2.2 Evaluation in the transverse direction

Figures 9 and 10 show the variation of the angular frequency and wave speed with the creep rupture time using the 10-, 15-, and 20-MHz probes. Almost no consistent trend is observed in these figures. One of the reasons for this is the short processing distance because of the relatively small thickness in the perpendicular direction. Another reason is that the creep damage was relatively small in the loading direction. This was also reflected in the models proposed by Tomohiro.[2] A thicker testing specimen would improve the sensitivity in the perpendicular direction.

5. Conclusions

Creep-tested 316LN SS samples were examined to study the creep damage using ultrasonic waves traveling in the direction of and perpendicular to the loading. The following conclusions were drawn.

1) By analyzing the angular frequency and wave speed of ultrasonic waves in the loading direction, we found that the angular frequency decreased with increasing creep time when 15- and 20-MHz contact transducers were used. Hence, the creep damage could be evaluated based on the angular frequency.
2) The wave speed also decreased with increasing creep rupture time, which made it possible to evaluate the creep damage from the wave speed. However, the degree of the changes in the wave speed was smaller than that of the angular frequency.
3) Almost no change occurred in either the angular frequency or the wave speed of the ultrasonic waves perpendicular to the direction of loading. This suggests that the waves in this direction were not sensitive enough to evaluate the creep damage, which also showed no systematic variations with the creep rupture time.

ACKNOWLEDGMENT

This research was supported by the Soongsil University (Seoul, Korea) Research Fund.

REFERENCES

1. Lee, S. G. and Chung, M. H., "Creep Damage Evaluation of High-Temperature Pipeline Material for Fossil Power Plant by Ultrasonic Test Method," Korean Society of Ocean Engineers, Vol. 13, No. 2, pp. 99–107, 1999.
2. Morishita, T. and Hirao, M., "Creep Damage Modeling Based on Ultrasonic Velocities in Copper," International Journal of Solids and Structures, Vol. 34, No. 10, pp. 1169–1182, 1997.
3. Kwak, D. S., Kim, S. H. and Oh, T. Y., "Effect of a Single Applied Overload on Fatigue Crack Growth Behavior in Laser-welded Sheet Metal," International Journal of Precision Engineering and Manufacturing, Vol. 7, No. 3, pp. 30–34, 2006.
4. Isobe, H., Fushimi, M., Ootsuka, M. and Kyusojin, A., "Non-contact Transportation of Flat Panel Substrate by Combined Ultrasonic Acoustic Viscous and Aerostatic Forces," International Journal of Precision Engineering and Manufacturing, Vol. 8, No. 2, pp. 44–48, 2007.
5. Kim, H. I., Seck, C. S. and Kim, J. P., "A Study on Nondestructive Evaluation Material Properties," Journal of the Korean Society for Precision Engineering, Vol. 22, No. 3, pp. 130–136, 2005.
6. Matsubara, S., Yokono, Y. and Imanaka, T., "Diagnosis of Material Degradation by Ultrasonic Waves," Japanese Society for Nondestructive Inspection, Vol. 46, No. 3, pp. 185–190, 1997.
7. Kumar, N. and Panakkal, J. P., "Analysis of Ultrasonic Velocity–Porosity Data in Polycrystalline Materials Using Rotation–Iteration Technique," Journal of Materials Science, Vol. 34, No. 19, pp. 4811–4814, 1999.
8. Kim, J. P. and Seok, C. S., "A Study on the Evaluation of Material Degradation of 1Cr-1Mo-0.25V Steel Using Ultrasonic Techniques," Transactions of the Korean Society of Mechanical Engineers A, Vol. 25, No. 12, pp. 2116–2124, 2001.
9. Lester, W. and Schmerr, Jr., "Fundamentals of Ultrasonic Nondestructive Evaluation: A Modeling Approach," Springer, pp. 283–304, 1998.
10. Fukuhara, H., Shinyya, N. and Kyono, J., "Detection of Creep Damage by Ultrasonic Waves," Japanese Society for Nondestructive Inspection, Vol. 40, No. 7, pp. 450–455, 1991.
11. Oh, S. W., Park, K. D., Kang, S. H. and Park, I. S., "The Steady-State Creep Rate and Creep-Rupture Life of 2024 Al Alloy at High Temperature," Transactions of the Korean Society of Mechanical Engineers, Vol. 12, No. 3, pp. 513–519, 1988.
12. Viswanathan, R., "Damage Mechanisms and Life Assessment of High-Temperature Components," ASM International, pp. 61–65, 1989.
13. ASTM, "Standard Guide for Evaluating Characteristics of Ultrasonic Search Units," E1065-99, 1999.
14. ASTM, "Standard Terminology for Nondestructive Examinations," E1316-06, 2006.